Tectonophysics 840 (2022) 229549

Contents lists available at ScienceDirect

Tectonophysics

journal homepage: www.elsevier.com/locate/tecto

New SKS splitting anisotropy measurements point to tearing beneath Central Italy

S. Pondrelli [a,*], J.M. Confal [a], P. Baccheschi [b]

[a] INGV, Sezione di Bologna, Bologna, Italy
[b] INGV, ONT, Rome, Italy

ARTICLE INFO

Keywords:
Seismic anisotropy
Mantle flows
Geodynamic model
Apennines
Central Mediterranean

ABSTRACT

In the middle of the Mediterranean, the partly still active Apennines subduction system has been usually defined using tomographic images and available shear wave splitting measurements. In this paper we describe the new seismic anisotropy dataset for Central Italy, the region where the transition between Northern and Southern Apennines occurs. The new measurements show NW-SE fast polarisation directions beneath the belt, due to the retreat of the slab, NN*E*-SSW orientations from proper Adriatic mantle sources, and E-W directed anisotropy, attributed to mantle convection flow at the Thyrranian side. Additionally, the new data suggest the presence of a toroidal mantle flow through a tear in the Apenninic slab, from the Adria to the Tyrrhenian side. However, mantle circulation and flows, identified by the pattern of shear wave splitting results, seem different from what was proposed in previous geodynamic models. Indeed, our results support the presence of a vertical slab tear with limited dimension. In the geodynamic model we propose, the tear acts to accommodate a differential slab retreat. The slab partitioning results in a different pattern and strength of seismic anisotropy traced from the Central Apennines with respect to the adjacent Northern and Southern Apennines.

1. Introduction

Central Italy marks the transition from the Northern to the Southern Apennines. This collisional belt characterises the entire Italian peninsula, running from the Po Plain to Sicily, and was built up as a consequence of the westward subduction of the Adria microplate beneath the present-day Tyrrhenian Sea, a back arc extensional basin resulting from the eastward slab rollback and related trench migration (Fig. 1).

Several tomographic studies, available for Italy and the surrounding regions, show the presence of slabs at depth (Wortel and Spakman, 2000; Piromallo and Morelli, 2003; Benoit et al., 2011; Giacomuzzi et al., 2011, 2012; Rappisi et al., 2022). In particular, beneath the Apennines, a high velocity body dipping towards the Tyrrhenian Sea is well identified by regional and local studies as a dipping slab; the open questions about it are mainly related to the presence and dimensions of slab windows or tears, especially beneath Central Italy. In Wortel and Spakman (2000) and Piromallo and Morelli (2003) these discontinuities in the slab seem to be laterally quite large. In Giacomuzzi et al. (2012) the Vs high anomaly is fragmented by relatively lower Vs values, interpreted as tears based on the high d(Vp/Vs) values detected at the same points at mantle depth. Rosenbaum et al. (2008) used tomographic images and magmatism studies to relate the supposed tears and break-offs of the slab to the kinematic reconstruction of the Apennines evolution. Benoit et al. (2011) see a complete termination of the slab beneath the northern Apennines at 43° latitude and beyond 300 km of depth, while other tomography studies (e.g. Lucente et al., 1999; Piromallo and Morelli, 2003; Rappisi et al., 2022) see a shallow discontinuity (above 200 km) with very low Vp values and a continuous slab down to depths beyond 400 km. In Chiarabba et al. (2020) receiver function profiles, low dVs, high d(Vp/Vs) ratio, high temperature, together with a widespread degassing support the heterogeneity attributed to the uppermost mantle. The Authors describe all these seismic observables hypothesising the occurrence of a mantle upwelling that follows a continental lithosphere detachment beneath the Central Apennines region. Also, the results obtained in this study allow the definition of a possible slab window more accurately, imaging the top of the residual descending slab at a depth lower than 100 km.

Usually, mantle flows sourced in discontinuities of slabs are supported by seismic anisotropy measurements, mainly SKS shear wave splittings, where the fast anisotropy directions are interpreted as due to olivine alignment caused by the mantle deforming along toroidal flows through or around slab windows or tears. Despite the denser dataset

* Corresponding author.
E-mail address: silvia.pondrelli@ingv.it (S. Pondrelli).

https://doi.org/10.1016/j.tecto.2022.229549
Received 20 April 2022; Received in revised form 22 July 2022; Accepted 23 August 2022
Available online 27 August 2022

already existing for the Northern Apennines (Salimbeni et al., 2007, 2008, 2013) and from the Southern Apennines to Sicily, in Central Italy only few seismic anisotropy measurements are available, thanks to CAP and SAP (Central and Southern Apennines Profiles) early temporary experiments and from few permanent stations (Margheriti et al., 2003). Beneath the Southern Tyrrhenian Sea and Sicily, seismic anisotropy data (Civello and Margheriti, 2004; Baccheschi et al., 2007) revealed a toroidal flow through the clearly detected slab tear. SKS splitting measurements available for the Southern Apennines show a nearly homogeneous pattern, following the strike of the belt and attributed to the mantle beneath the retreating slab. The absence of seismic anisotropy supporting a mantle flow through the slab leads to the idea that an existing slab tear or window is not large enough to favour any flows or the mantle material reorganisation is in an early stage of deformation, not well developed yet (Baccheschi et al., 2007; 2008; Baccheschi et al., 2011). On the contrary, any suggestions of mantle flow beneath the Central Apennines has mainly been supported by tomographic results, lacking in SKS splitting measurements due to the poor seismic anisotropy dataset (i.e. Lucente et al., 2006; Jolivet et al., 2009; Giacomuzzi et al., 2012).

In this study new shear wave splitting measurements fill the gap existing beneath the Central Apennines, thus enriching the already wealthy dataset for the Italian peninsula (Pondrelli et al., 2022). Together with the previous, new measurements are here used to shed some more light on the mantle circulation beneath the study region and on possible mantle flow that would better support the presence and dimensions of slab windows or tears.

2. Geodynamics and tectonics of the Central Apennines

The Central Apennines is part of the arcuate Apennines chain, a single-verging belt running from northwestern Italy down throughout the peninsula, continuing to the southwest into Sicily and merging into the Maghrebides in northwestern Africa (Malinverno and Ryan, 1986; Faccenna et al., 2001 and references therein). The geodynamic evolution of this sector of the chain was guided, during the Neogene, by the collision and convergence between the Adria microplate, Africa promontory, and the European plate (Dewey et al., 1989; Picotti et al., 2014) and accreted from the Miocene to Early Pleistocene during the westward-directed subduction of the Adriatic–Ionian lithospheric slab (Malinverno and Ryan, 1986; Patacca et al., 1990). Starting in the Late Miocene, the central portion of the Apennines was involved in the evolution of a post-collisional orogenic system, with thrust-belt and foredeep migrating towards more external domains (Fig. 1). Extensional tectonics associated to the rollback of the Ionian portion of the subducting lithosphere progressively migrated from the western to the eastern parts of the orogen, producing crustal thinning and ocean-floor spreading in the Southern Tyrrhenian Sea and pushing the Apennines belt to the east (Malinverno and Ryan, 1986; Rosenbaum et al., 2008). The belt migrated northeastward in the Northern Apennines, eastward in the Central and Southern Apennines, and southeastward in Calabria and Sicily; to the east, the Adria margin served as the foreland to the migrating thrust belt. This process acted in the presence of the active subduction (i.e. the Adria–Ionian lithospheric slab) extended from Sicily to the Northern Apennines, as revealed by tomographic studies (Lucente et al., 1999; Piromallo and Morelli, 2003; Giacomuzzi et al., 2011), that evolved in a delamination process at least in the northern part of the Apennines when the subducting oceanic crust consumed early (e.g., Chiarabba et al., 2014).

3. Data and methods

SKS phases recorded by 76 stations have been analysed using SplitRacer (Reiss and Rümpker, 2017) (Fig. 2 and Table 1). We selected the seismograms of earthquakes with a magnitude greater than 6.0, with an epicentral distance between 85° and 140°, and occurred between 2010 and 2020 (1618 events in total). Most of the data are from stations of the Italian National Network (IV, Rete Sismica Nazionale, 2006; http://terremoti.ingv.it/instruments/network/IV). Moreover, data recorded at some stations of the MedNet network (MN, Mediterranean Very Broadband Seismographic Network (MedNet), 1990; http://terremoti.ingv.it/instruments/network/MN) and stations belonging to the Regional Seismic Network of North Western Italy Data set (GU; http://terremoti.ingv.it/instruments/network/GU) also contribute to the final results (Table 1).

To perform the shear wave splitting analysis and get the fast

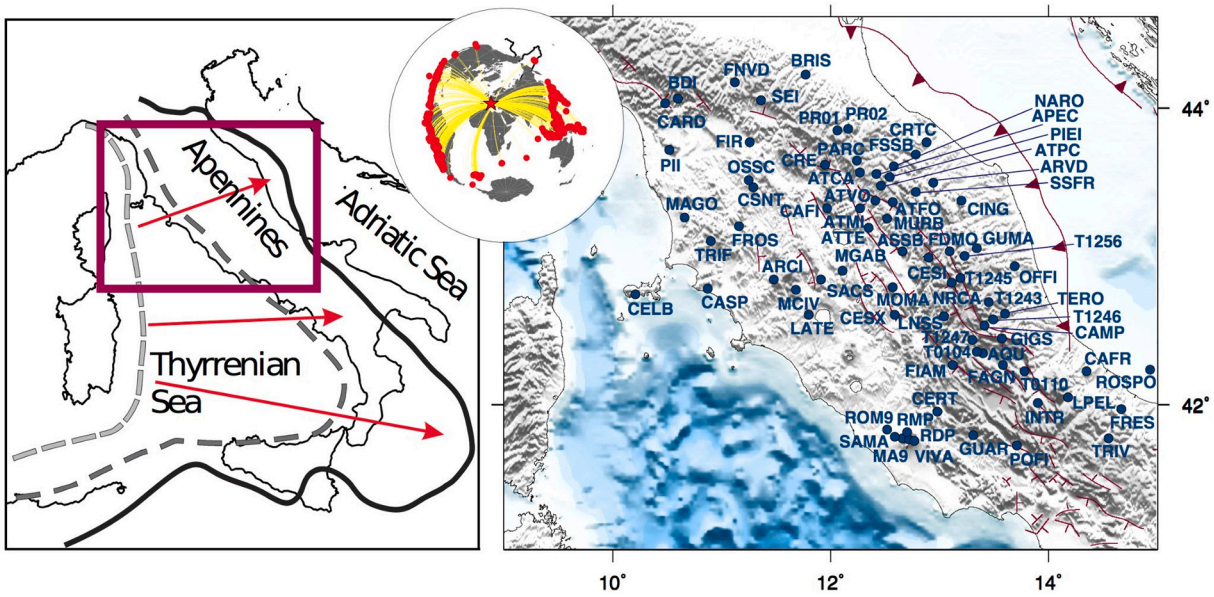

Fig. 1. Left: sketch of the geodynamic environment of the study region (brown red box). The thick black line represents the present-day location of the subduction trench, while the dashed grey lines are its past position at two stages of the slab retreat (Faccenna et al., 2001). Red arrows represent direction and amount of trench retreat. Right: map of used stations and main tectonic features (brown red notched line represents the present day subduction trench, simple lines are the Apenninic extensional structures). Top centre: distribution of analysed earthquakes. (For interpretation of the references to colour in this figure legend, the reader is referred to the web version of this article.)

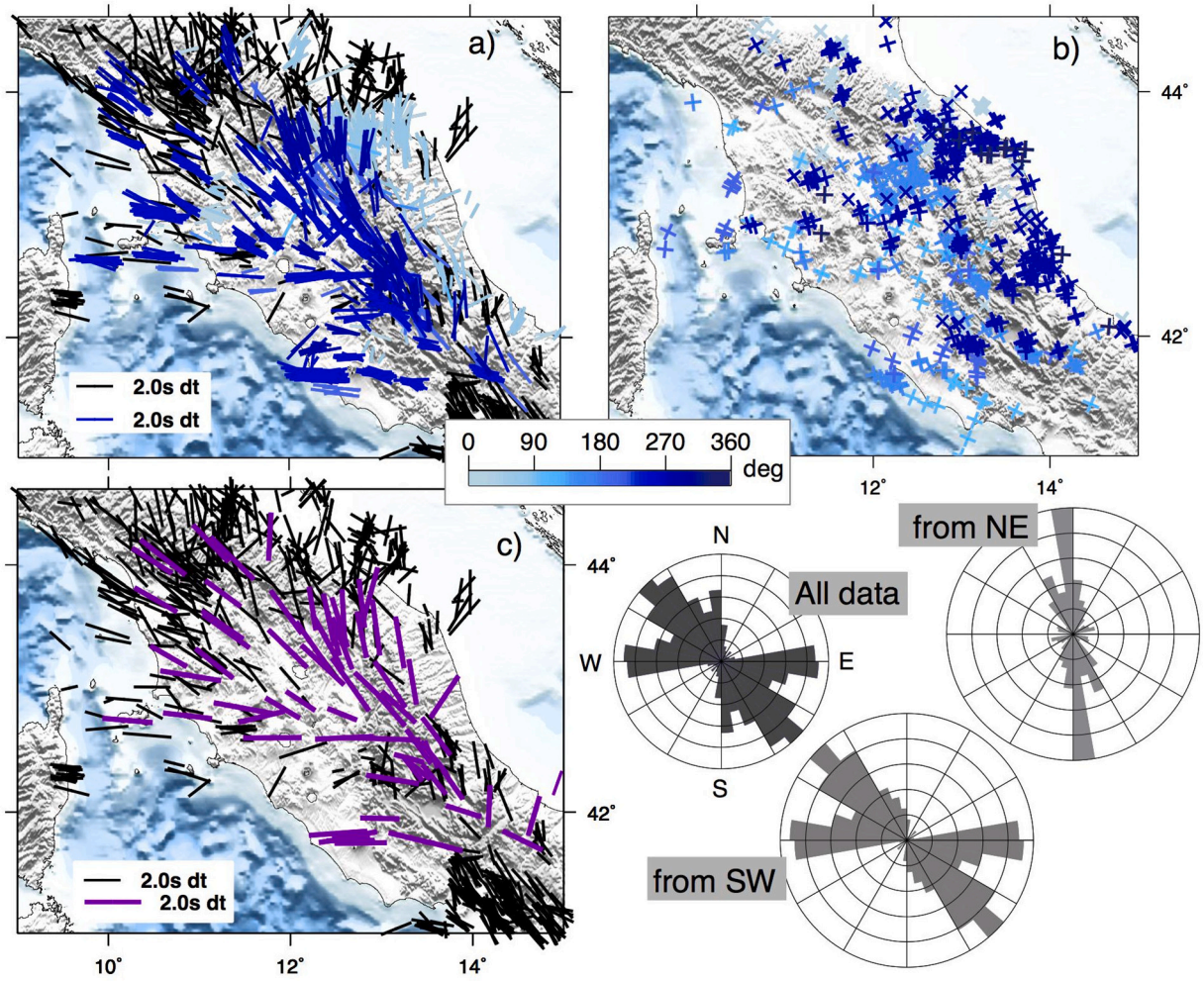

Fig. 2. a) Map of new individual SKS splitting measurements (colored as a function of back-azimuths) plotted at the 150 depth piercing point; b) null measurements; c) average values of new measurements at each station, computed from a number of data greater than 3. In the background, black symbols are previous measurements (Pondrelli et al., 2022); d) rose diagrams of all new measurements (top left) and of data with a NE (top right) or SW (bottom centre) back-azimuth. (For interpretation of the references to colour in this figure legend, the reader is referred to the web version of this article.)

polarisation direction and the delay time, we used the code SplitRacer (Reiss and Rümpker, 2017), based on the Silver and Chan (1991) and thus on the minimization of the energy on the transverse component. Shear wave splitting measurements are obtained supposing that the detected anisotropy has a horizontal symmetry axis. SplitRacer has been chosen because it is particularly useful in the selection and preprocessing of seismic waveforms and because it is able to identify possible sensor misalignments. Compared to other studies, error estimates might be larger, due to the degree-of-freedom formulation and the 95% confidence level stacking method (Reiss et al., 2019). All signals have been band-pass filtered between 7 and 20 s, analysed only when SNR was greater than 3. The measurements have been repeated for every signal in 40 time windows to get well constrained uncertainties. Substantially, mostly SKS- and few SKKS-waveforms have been analysed.

SKS splitting measurements have been classified (following the SplitRacer nomenclature) as good, if the energy reduction is greater than 80%, the error in the fast direction was approximately ±25° and in the delay time ±0.6 s; average, if the energy reduction is greater than 60%, the error in the fast direction was approximately ±60° and delay time ±1.5 s. Waveforms containing other phases in the SKS (SKKS) arrival window were discarded and the mean 95% confidence level had to be well defined. Moreover, only measurements with a delay time lower than or equal to 3 s are considered (Lopes et al., 2020; Reiss et al., 2019). Data are classified as nulls when SKS polarisation is almost linear in the radial component and when the transversal component does not show any energy. The absence of energy usually corresponds to a null measurement, that reflects either a lack of anisotropy, a propagation along the anisotropic symmetry axis, or a propagation along multilayer anisotropic structures with a summary zero effect on the waveform.

4. Results

In Fig. 2 the 1776 new good measurements at 76 stations are shown, including 1122 SKS splitting (574 good and 548 average) and 654 null measurements (Files SM1 and SM2 in Supplementary Material). We have 1 to 46 SKS measurements per station, with an average of about 15 for each of them (Table 1 and Fig. 2). For the entire splitting dataset the mean delay time is of 1.7 s, with an error of ±1.0 s and the mean fast polarisation error is ±19°. Most of the selected measurements (43.3%, 486 measurements) show a NW-SE direction (110–155°), with a mean delay time of 1.6 s. About 24.2% (271 measurements) splitting measurements have a N-S to NNE-SSW fast axis (−20–45° or 160–225°), with a mean delay time of 1.6 s, while almost the same amount of results (25.2%, 283 measurements) are E-W directed (75–105°), but with the highest mean delay time of 1.8 s. The remaining small amount of data (7.3%, 82 measurements) without any well-recognized fast axes orientation has a smaller mean time delay, about 1.5 s.

Table 1
Station list.

Station and Net	Lat. (°)	Long. (°)	Average FPD (° from N)	FPD error	Average Delay Time (s)	Delay Time error	n. of data
APEC IV	43.56	12.42	−11.93	0.76	1.91	0.75	33
AQU MN	42.35	13.40	−51.18	0.52	1.06	0.39	72
ARCI IV	42.85	11.48	−79.49	0.61	2.15	0.58	15
ARVD IV	43.50	12.94	−7.58	0.67	2.01	0.61	84
ASSB IV	43.04	12.66	−35.12	0.91	2.31	0.27	14
ATCA IV	43.57	12.27	−33.00	0.90	1.54	0.78	2
ATFO IV	43.37	12.57	−20.94	0.61	1.98	0.69	33
ATMI IV	43.33	12.27	−34.86	0.88	2.36	0.45	15
ATPC IV	43.48	12.46	−15.21	0.78	1.92	0.57	38
ATTE IV	43.20	12.35	−46.87	0.90	2.11	0.37	19
ATVO IV	43.38	12.41	−28.59	0.82	2.23	0.47	22
BDI IV	44.06	10.60	−51.88	0.77	2.06	0.57	27
BRIS IV	44.22	11.77	2.94	0.60	1.70	0.49	28
CAFI IV	43.33	11.97	−45.44	0.87	1.93	0.65	24
CAFR IV	42.23	14.35	−11.00	0.97	2.15	0.03	2
CAMP IV	42.54	13.41	−35.70	0.37	1.49	0.37	66
CARD GU	44.03	10.48	−57.47	0.96	1.69	0.35	9
CASP IV	42.79	10.87	−83.32	0.83	1.75	0.54	56
CELB IV	42.75	10.21	−85.02	0.93	1.79	0.44	34
CERT IV	41.95	12.98	−88.59	0.61	1.36	0.42	25
CESI IV	43.00	12.90	−46.06	0.56	1.76	0.63	27
CESX IV	42.61	12.59	87.38	0.83	2.10	0.51	46
CING IV	43.38	13.20	−9.43	0.61	1.88	0.53	33
CRE IV	43.62	11.95	−35.64	0.82	1.90	0.65	13
CRTC IV	43.77	12.88	15.42	0.74	1.94	0.43	5
CSNT IV	43.47	11.29	−54.19	0.83	2.04	0.31	19
FAGN IV	42.27	13.58	−38.35	0.72	1.34	0.58	33
FDMO IV	43.04	13.09	−33.63	0.71	1.98	0.67	55
FIAM IV	42.27	13.12	−80.62	0.50	1.90	0.57	21
FIR IV	43.77	11.26	−53.66	0.94	1.57	0.18	25
FNVD IV	44.17	11.12	−43.76	0.64	1.82	0.70	14
FRES IV	41.97	14.67	16.31	0.43	1.44	0.88	5
FROS IV	43.21	11.16	−51.48	0.98	1.73	0.34	24
FSSB IV	43.69	12.78	−6.61	0.87	1.77	0.50	18
GIGS IV	42.45	13.57	−38.43	0.84	1.43	0.48	24
GUAR IV	41.79	13.31	−76.23	0.95	1.55	0.43	21
GUMA IV	43.06	13.34	−9.49	0.40	1.63	0.76	10
INTR IV	42.01	13.90	−72.21	0.48	1.28	0.39	14
LATE IV	42.61	11.80	89.67	0.99	2.10	0.49	6
LNSS IV	42.60	13.04	−87.95	0.89	2.51	0.28	7
LPEL IV	42.05	14.18	2.51	0.59	1.50	0.52	21
MA9 IV	41.77	12.66	89.33	0.85	1.71	0.44	16
MAGO IV	43.27	10.66	−60.01	0.99	1.49	0.30	4
MCIV IV	42.78	11.68	76.40	1.00	1.68	0.64	5
MGAB IV	42.91	12.11	−56.51	0.88	1.22	0.22	32
MOMA IV	42.80	12.57	−68.10	0.74	1.11	0.29	10
MURB IV	43.26	12.52	−3.01	0.99	0.93	0.44	3
NARO IV	43.61	12.58	−3.10	0.76	1.76	0.45	7
NRCA IV	42.83	13.11	−41.30	0.65	1.44	0.36	40
OFFI IV	42.94	13.69	33.60	0.36	1.80	0.79	7
OSSC IV	43.52	11.25	−55.53	0.92	1.80	0.37	7
PARC IV	43.65	12.24	−8.94	0.98	1.58	0.49	20
PIEI IV	43.54	12.54	−17.55	0.83	1.88	0.59	22
PII IV	43.72	10.52	−60.14	0.93	1.76	0.39	14
POFI IV	41.72	13.71	−75.27	0.94	1.17	0.38	20
PR01 IV	43.85	12.06	23.00	1.00	–	–	1
PR02 IV	43.86	12.16	67.00	1.00	–	–	1
RDP IV	41.76	12.72	−87.77	0.77	1.32	0.44	9
RMP IV	41.81	12.70	81.11	0.87	1.60	0.63	28
ROM9 IV	41.83	12.52	85.86	0.52	2.08	0.61	15
ROSPO IV	42.24	14.93	19.50	0.97	0.87	0.15	2
SACS IV	42.85	11.91	−59.00	0.93	1.40	0.31	31
SAMA IV	41.78	12.59	82.07	0.79	1.84	0.70	19
SEI IV	44.05	11.36	−45.38	0.58	2.16	0.65	10
SSFR IV	43.44	12.78	−11.79	0.87	1.68	0.52	26
T0104 IV	42.36	13.34	−38.13	0.50	1.12	0.34	17
T0110 IV	42.23	13.78	−34.62	0.81	1.25	0.40	38
T1243 IV	42.70	13.45	–	–	–	–	1
T1245 IV	42.86	13.19	−47.00	0.93	1.64	0.32	4
T1246 IV	42.58	13.49	−22.00	0.79	2.10	0.15	2
T1247 IV	42.44	13.30	−74.94	0.80	1.08	0.17	8
T1256 IV	43.01	13.23	–	–	–	–	1
TERO IV	42.62	13.60	−36.94	0.86	1.67	0.42	40
TRIF IV	43.11	10.90	−80.71	0.92	2.20	0.75	39
TRIV IV	41.77	14.55	−63.87	0.55	1.58	0.47	30
VIVA IV	41.75	12.77	89.18	0.99	1.88	0.41	16

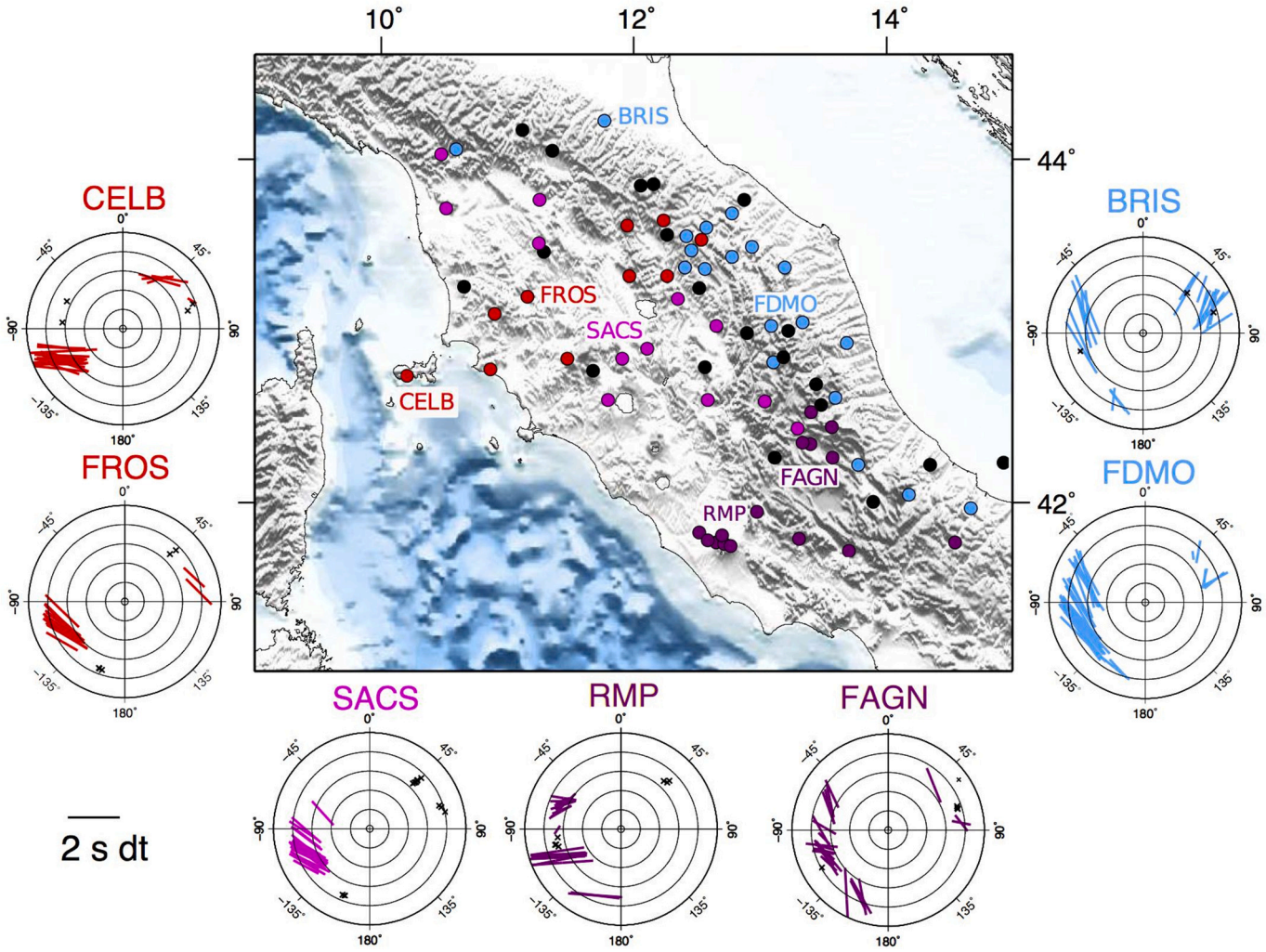

Fig. 3. Map with stations colored on the basis of different patterns revealed in polar plots. Around the map, some polar plots show the examples of recognized patterns. In red, are reported stations at which back-azimuthal dependence is absent; in pink, cases where for eastern back-azimuths null measurements only are obtained; stations where a clear back-azimuthal dependence is present are mapped in light blue; in purple, the locations where a group of *E*-W fast polarisation directions is detected only in the SW quarter of back-azimuthal origin. (For interpretation of the references to colour in this figure legend, the reader is referred to the web version of this article.)

4.1. Anisotropy pattern of Central Italy

Previous studies on seismic anisotropy in the Apennines show that most of the available splitting measurements are distributed in the Northern and Southern Apennines. Only a few of them were available for the central sector of the belt. In this study, we fill the gap (Fig. 2) in the transition zone between the Northern and Southern Apennines. New data show different directions, but the NW-SE pattern parallel to the Apenninic belt prevails (Fig. 2a and b). Additionally, we identified other directions, such as the E-W pattern, frequent on the Tyrrhenian side, as well as the N-S to NNE-SSW directions, mainly related to the outer part of the belt, namely the Adriatic side.

Earlier studies on seismic anisotropy, focused on neighbouring regions, show a clear back-azimuthal dependence of fast directions (Plomerová et al., 2006; Salimbeni et al., 2007, 2008, 2013, 2022). This feature is visible in Fig. 2a, where shear wave splitting data are mapped and colour scaled with back-azimuth, and it is also confirmed by the rose diagrams showing the frequency of the data in the same back-azimuth interval (Fig. 2). SW back-azimuth fast polarisation directions are mainly Apenninic, thus N*E*-SW directed, but also show a contribution of E-W measurements. NE back-azimuth measurements show a clear prevalence of a N-S trend, the direction usually attributed to a proper Adria mantle domain (Salimbeni et al., 2013, 2022).

However, the back-azimuthal dependency is not recognizable everywhere. New measurements do not show any typical periodicities with back-azimuth, usually attributed to double layer, multilayer, or dipping structure (e.g. Silver and Savage, 1994). Nevertheless, some interesting patterns are found, evidenced by polar plots produced at each station (Figure 1SM in Supplementary Material). In several locations, measurements show a homogeneous pattern with respect to the back-azimuth, mainly on the Tyrrhenian side (red data in Fig. 3). Such data distribution is typical of the absence of lateral variation of the anisotropy beneath the station. On the contrary, on the Adriatic side a back-azimuthal dependence is clearly identified (light blue data in Fig. 3). This pattern supports the presence of lateral variations, in particular different anisotropy domains in the east and west beneath the stations. Another pattern is found at several stations in the transition zone from the Tyrrhenian side to the chain, characterised by only nulls for events with E back-azimuths (pink data in Fig. 3). In this case, we just take into account that the seismic rays coming from the west crossed a different structure with respect to those coming from the east. The latter is a pattern identified at several stations located in the southwestern part of the study region, where a considerable amount of *E*-W fast polarisation directions are detected only in the SW quarter of back-azimuths.

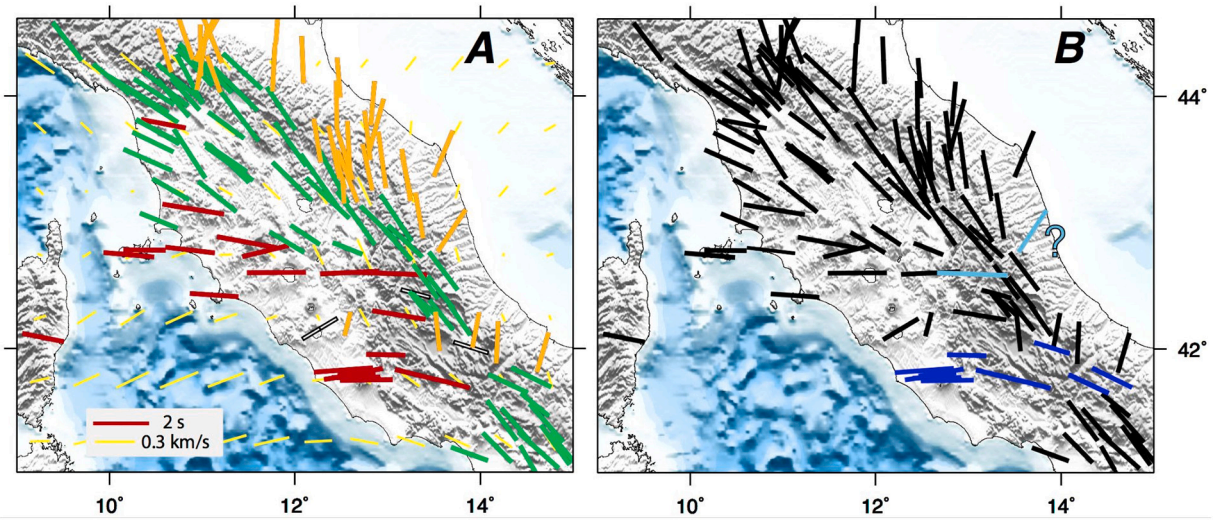

Fig. 4. A: map of all available average values for new and previous shear wave splitting measurements for this region, drawn with different colours as a function of the fast polarisation direction: red is used for data with a 75°-105° direction; green is for those with a 110°-155° direction; orange for those with −20°- 45° direction. In the background, in yellow, the Pn anisotropy directions are plotted (from Díaz et al., 2013). B: the same data reported on the left, with in blue, the measurements interpreted to indicate a mantle flow and in light blue measurements that may induce a similar interpretation, but insufficient to do so. (For interpretation of the references to colour in this figure legend, the reader is referred to the web version of this article.)

This feature becomes weaker (i.e. the delay time decreases) moving into the belt (purple data in Fig. 3). This represents a peculiar pattern that is strongly related to this region.

Average values computed at each station are mapped in Fig. 2c, where the identified pattern perfectly reconciles with previous measurements available in the north and south sector of the study region. The NW-SE Apenninic pattern of fast direction coincides mostly with the highest part of the chain, while E-W average fast polarisation directions characterise the Tyrrhenian side. In the Adria side of the belt, N-S to NE-SW fast directions are identified, showing a more scattered distribution. Average values show a clear transition moving from north to south. In the Northern Apennines, north of 43° of latitude, average anisotropy directions are oriented NW-SE, well in agreement with the strike of the belt along the topographical high and in the western part, while homogeneously N-S to NNE-SSW pattern of fast axes are recognized on the eastern flank of the chain. South of 43° of latitude, E-W fast polarisation direction strongly dominates on the Tyrrhenian side and enters the chain up to the topographical high. Here a thinner band of NW-SE average values is also found, in continuity with the typical Apenninic trend; it seems to shortly interrupt at 42.1° of latitude however and then reappears south of 41.9° (Figs. 2c and 4). In correspondence with this change, the typical N-S to NNE-SSW Adriatic characteristic direction is present also within the belt domain, as well as to the east where it is commonly detected along the Adriatic Sea side. These differences may also be appreciated in Fig. 5, where the fast polarisation directions and delay times across and along the chain are reported along cross sections oriented perpendicular to the belt (n-n',c-c', and s-s'). In some parts of the transects, two patterns of fast axes coexist. Beneath the highest part of the belt, the NW-SE Apenninic trend (green symbols) is present along with the NNE-SSW Adriatic trend (orange symbols). This feature is visible especially on the n-n' section in correspondence of the topographical high, with very high time delays. Following the transects from west to east, average time delays (purple squares) are about 2 s on the Tyrrhenian side, then they decrease to 1–1.5 s and reach up to 2.2 s, in correspondence to the highest portion of the belt. Lower values of average delay times (1.2–1.5 s) are found on the Adriatic side. On the belt-parallel transect (a-a') a clear uniform trend of averaged fast polarizations between 130 and 170° is visible, while the time delay seems to increase from south to north.

5. Discussion

Shear wave splitting measurements are characterised by a good horizontal resolution, but not a vertical one; SKS measurements indeed should be read as the integral of all the anisotropy crossed by the seismic ray. Consequently, it is difficult to define the depth location of the detected anisotropy. Moreover, the new measurements show an interesting back-azimuthal dependence pattern, but none of the typical periodicities related to multilayer or dipping anisotropy. This is in agreement with the results of previous trials to relate shear wave splitting measurements to complex anisotropic structures at some stations located in the northern part of our study region (Salimbeni et al., 2014). The study region belongs to an active geodynamic place, characterised by a late stage subduction, where it is common to have strong lateral changes of the anisotropy in a short distance, due to a slab that works as a discontinuity between different domains. Following these premises, the interpretation mainly focuses on the lateral variations of the detected anisotropy, i.e. mantle above or below the slab and possible mantle flows. To link the seismic anisotropy identified in this study to what we already know of the structure at depth, we compare this data with other seismic anisotropy measurements and with available tomographic images.

5.1. Comparison with Pn anisotropy measurements

In Fig. 4, together with all available average splitting values for the Central Apennines (this paper and Pondrelli et al., 2022), Pn anisotropy by Díaz et al. (2013) is mapped. Pn seismic anisotropy is representative of the shallow lithospheric mantle, immediately below the Moho. From this comparison we can assume that in regions where different seismic anisotropy data agrees, we have the same pattern in the lithospheric and asthenospheric mantle, that is a coherent pattern with depth. This assumption could not be valid where a discrepancy between SKS shear wave splitting data and Pn exists, as in the southern part of our study region. Due to the lower horizontal resolution of Pn anisotropy data, we compare it with average fast polarisation values. Pn anisotropy and shear wave splitting measurements show a good agreement in terms of fast direction in Tuscany and along the belt, where the typical NW-SE Apenninic direction is detected. A rather good correspondence is also identified all along the Adriatic side. On the other hand, we see opposing

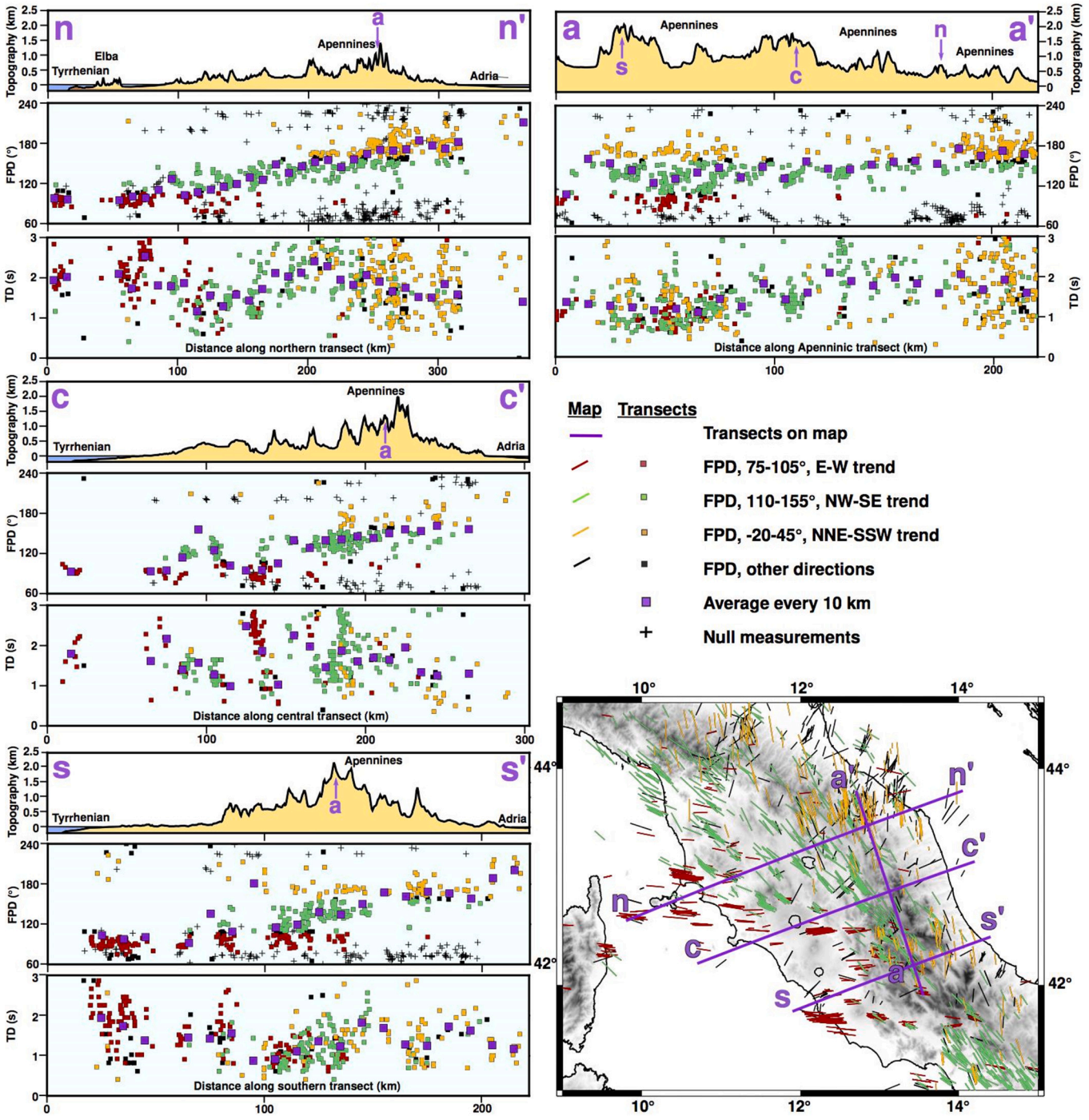

Fig. 5. Four transects of 80 km width, showing new and old fast polarisation directions (FPD) and time delay (TD) measurements, colour coded according to E-W, NW-SE and NNE-SSW fast polarisation directions, with topographic profiles on top. Three profiles are perpendicular (n-n',c-c',s-s') to the Apenninic belt and one is parallel (a-a') to it. Along the transects average values of time delay and fast polarisation directions were calculated every 10 km (purple squares). The map in the lower right corner shows the locations of the transects (purple lines) and splitting measurements, with the length of the vectors according to the time delay (2 s in the legend). (For interpretation of the references to colour in this figure legend, the reader is referred to the web version of this article.)

fast polarisation direction patterns on the Tyrrhenian side south of 43° of latitude, where *E*-W SKS shear wave splitting measurements cut nearly perpendicularly the Pn measurements. This discrepancy allows us to hypothesize this E-W shear wave splitting data as related to an asthenospheric mantle source, while the NW-SE Pn anisotropy direction is connected to an Apenninic frozen deformation at lithospheric mantle depth.

5.2. Comparison with tomography images

It is well known that all tomographic studies imaging the Italian peninsula identify an abrupt change of dVs and/or dVp at 43° of latitude, interpreted as an interruption of the slab (e.g. Wortel and Spakman, 2000; Piromallo and Morelli, 2003; Benoit et al., 2011; Giacomuzzi et al., 2011; Rappisi et al., 2022). However, all these models show relevant differences south of 43° of latitude, e.g. different dimensions (including the vertical one) of the possible slab window. Among the

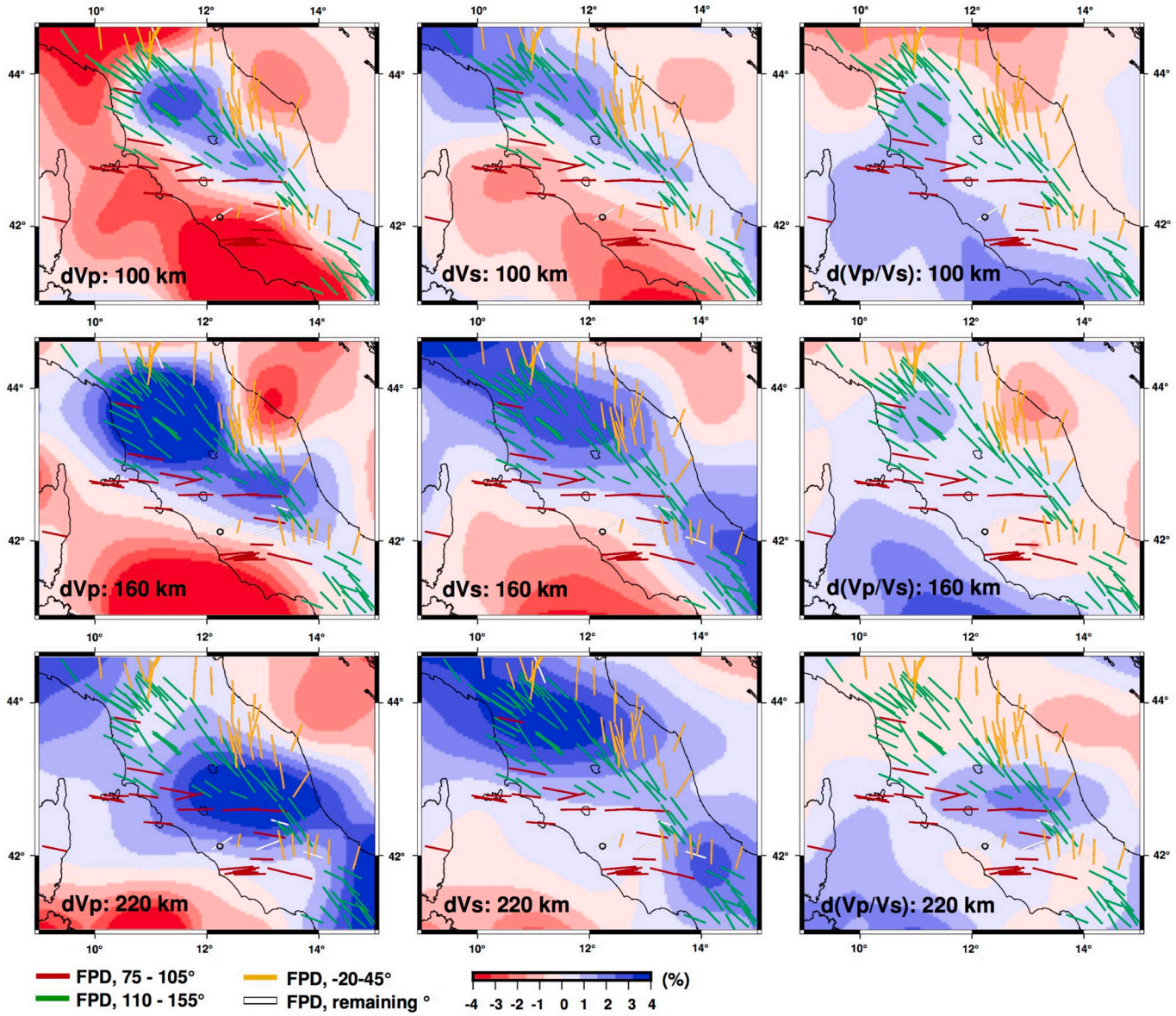

Fig. 6. Overlaps of average values of shear wave seismic anisotropy at stations, colored differently to enhance Apenninic NW-SE - green; Tyrrhenian nearly E-W - red; Adria N-S to NNE-SSW - orange directions, over tomographic images from Giacomuzzi et al. (2011 and 2012). Left: dVp, Central: dVs, Right: d(Vp/Vs). Top: 100 km, centre: 160 km, bottom: 220 km. The length of the splitting bars depends on the time delay, see Fig. 4. (For interpretation of the references to colour in this figure legend, the reader is referred to the web version of this article.)

available tomographic studies for the Italian peninsula, we selected Giacomuzzi et al. (2011, 2012) to compare with our measurements because it has a very good resolution in our study region. We mapped all available average splitting values at station sites over dVp, dVs and d (Vp/Vs) tomographic images at different depths (Fig. 6; 100, 160, and 220 km). In the comparison with P-wave velocity perturbations, we can observe, mainly at depths of 100 and 160 km, that NW-SE fast polarisation directions overlap in a convincing coherent pattern the high-velocity anomaly, that corresponds to the dipping slab towards the west beneath the Tyrrhenian Sea. E-W fast polarisation directions border the high velocity body on the western side and N-S to NE-SW fast polarisation directions do the same on the eastern side. This pattern changes at 42° of latitude, where the typical Apenninic fast polarisation directions are absent and E-W and N-S to NE-SW fast axes prevail in correspondence to a weakening of the high seismic velocity anomaly. The dVs high-velocity anomaly already weakens at about 43° of latitude in all depth layers, where E-W oriented fast polarisation directions are found, while at around 42° a new high-velocity anomaly starts. These heterogeneities of the high-velocity anomaly are interpreted as tears in a fragmented slab (Giacomuzzi et al., 2011, 2012 and references therein).

From the comparison of seismic anisotropy data with the d(Vp/Vs) maps, a striking feature is the good correspondence between *E*-W measurements and the positive d(Vp/Vs) anomaly, that Giacomuzzi et al. (2012) interpreted as possible upwellings of hot or hydrated mantle material. Such correspondences, already described for shallower layers, can also be recognized in the deeper layer, as shown at 220 km depth (Fig. 6, bottom row), in the dVs and d(Vp/Vs) maps.

5.3. *Interpretation*

Seismic anisotropy along the Apennines has been measured intensively and studied in great detail along the Northern Apenninic arc and along the southern part of this belt up to the Calabrian Arc and Sicily (Margheriti et al., 2003; Civello and Margheriti, 2004; Lucente et al.,

2006; Plomerová et al., 2006; Salimbeni et al., 2007, 2008, 2013, 2022; Baccheschi et al., 2007; 2008; Baccheschi et al., 2011). Data analysed in this study fill the gap of splitting measurements in the Central Apennines and allow to harmonise all the available interpretations given for the extremes of the belt.

All previous studies described the NW-SE shear wave splitting direction detected along the Northern Apennine chain as the mantle below the slab deformed by a fast slab rollback; the deformed mantle part is narrow (e.g. Salimbeni et al., 2007) and this characteristic is consistent with the new NW-SE measurements from this study. The prevalent N-S to NN*E*-SSW fast polarisation directions, measured all along the Adriatic coast, on the outer part of the belt, reinforce the hypothesis that they represent the pattern of the proper Adria mantle not deformed by the slab retreat, but possibly generated by the dragging forces (Salimbeni et al., 2013; Baccheschi et al., 2007). Indeed, the Adria plate moves to N-NE but also rotates in a counter-clockwise motion centred in a pole located in the Western Alps (Serpelloni et al., 2005; D'Agostino et al., 2008) and with rotation traces in agreement with shear wave splitting measurements directions. The transition between the NW-SE pattern below the slab and the proper Adria mantle has been identified (here and in previous studies) studying data of stations characterised by back-azimuthal dependence, that is where at the same station different directions of fast polarisation are detected from events with opposite back-azimuth. This is the case for stations plotted in light blue in Fig. 3, for which the polar plots show NW-SE fast polarisation directions detected by events with western back-azimuth and N-NE anisotropy directions from those coming from the east. The horizontal transition between the two domains clearly occurs beneath the outer part of the Apennines, where all stations with this feature are located (Fig. 4).

Another prevailing direction is the *E*-W fast polarisation found south of 43° of latitude and mainly located in the Tyrrhenian side (Fig. 4). E-W direction has been always related to the roll-back extensional tectonics that produced the opening of the Tyrrhenian Sea (10–5 Ma for the northern part and 6 Ma to present for the southern part, e.g., Rosenbaum and Lister, 2004; Chiarabba et al., 2005); *E*-W seismic anisotropy pattern would represent the mantle circulation above the slab (Lucente et al., 2006). This hypothesis could explain the pattern of fast directions observed in the central part of the Northern Apennines, where the slab roll back had its maximum retreat (Salimbeni et al., 2008). In the northernmost part of the Apennines, also on the Tyrrhenian (Tuscany) side, a NW-SE to WNW-ESE fast polarisation direction prevails. This pattern has been attributed to the asthenospheric flow coming from the Alpine sub slab mantle (Western Alps, Salimbeni et al., 2018), feeding the mantle flow along (and above) the northernmost portion of the slab and converging with the *E*-W mantle circulation in the centre of the Tyrrhenian Sea (Fig. 7). In this case, discriminating between the mantle flow above and below the slab could not be done based simply on the recognition of back-azimuthal dependence, because measurements have everywhere the same NW-SE direction. The distinguishing factor is the high velocity anomaly in tomographic images, i.e. the underplating Adria lithosphere position, which is substantially the same north of 43° of latitude in all tomographic models (e.g., Wortel and Spakman, 2000; Piromallo and Morelli, 2003; Benoit et al., 2011; Giacomuzzi et al., 2011; Giacomuzzi et al., 2012; Rappisi et al., 2022), accompanied by the gentle rotation of polarisation directions from NW-SE to WNW-ESE and E-W in the Tyrrhenian side.

However, the new measurements presented in this work show new features. Firstly, the E-W fast polarisation directions reach so far east below 43°, penetrating the "chain domain", exactly where tomographic images report discontinuities in the high dVp and dVs anomalies, interpreted as a possible slab tear (Figs. 6 and 7). By the way, at the same latitude, the typical NW-SE Apenninic pattern does not show any variation, confirming that the deformation due to the slab retreat is unmodified. Moreover, the measurements on the Adria side do not show any particular pattern given by possible mantle flows that we would expect in the direction from Adria mantle (squeezed by slab retreat) to the Tyrrhenian domain above the slab. The few measurements that may induce a similar interpretation are considered insufficient to support the presence of a mantle flow trough the slab because the Apenninic pattern is continuous and their direction is in agreement with similar data from the same domain (Fig. 4B). Consequently we suppose that the dimension of the slab discontinuity located here by tomographic studies, should be still too narrow to favour a mantle flow as relevant as possibly well detected with shear wave splitting measurements.

Immediately south, another interesting feature is the presence of some N-S and NN*E*-SSE fast polarisation directions distributed across the belt around 42° of latitude, where NW-SE along-chain data are absent (Fig. 4A and B). These data are surrounded by the easternmost *E*-W measurements. If we assume that these N-S and NNE-SSE measurements represent the undeformed Adria mantle, we can hypothesize that a small portion of the mantle beneath the Apennines did not undergo the slab retreat deformation as occurred north and south of this point. Moving further south of these N-S and NNE-SSE measurements, that we attribute to the Adria proper mantle, there is a set of data that may represent a toroidal mantle flow of limited dimensions from sub to supra slab mantle (Figs. 4B and 7): in the outer part of the Apennines, WNW-ESE average measurements converge with the *E*-W data in the Apennines and then, towards the west, also with data in the Tyrrhenian side. South of this possible mantle flow, all measurements realign with the NW-SE Apenninic anisotropy direction.

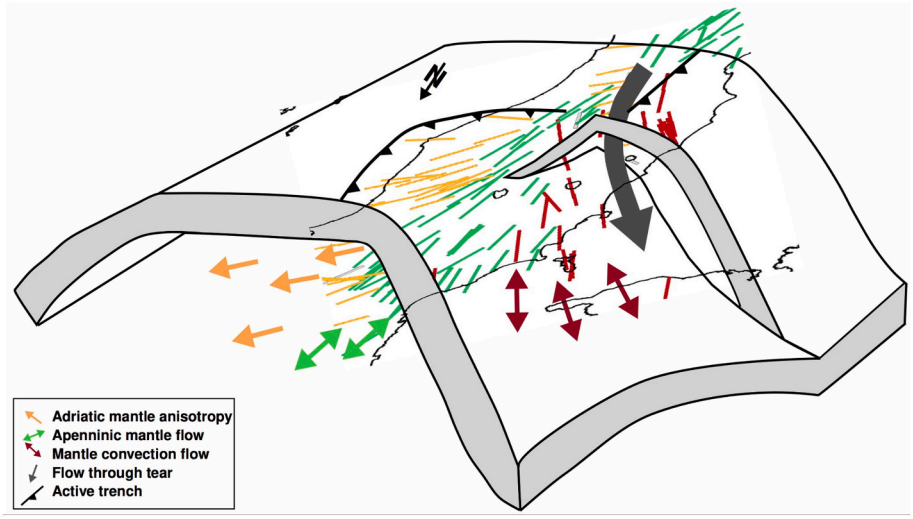

Fig. 7. Sketch of the possible mantle flows defined using seismic anisotropy directions and the shape of the slab from tomographic images (Giacomuzzi et al., 2011; Giacomuzzi et al., 2012). Possible location for an additional horizontal tear is after Chiarabba et al. (2020). On the top, average seismic anisotropy data are from Fig. 4. Colored arrows represent the interpreted mantle deformation and flows: yellow is the proper Adriatic mantle, light green represents the Apenninic mantle deformed by slab retreat, red arrows represent the mantle circulation above the slab and the dark grey arrow is the supposed mantle flow through a vertical slab tear. (For interpretation of the references to colour in this figure legend, the reader is referred to the web version of this article.)

All these new findings are synthesised in the sketch in Fig. 7. North and south of the Central Apennines region we find the same pattern recognized in previous studies. Moreover, the new measurements collected in this study show some differences that can allow us to formulate a renewed geodynamic model for the area. The seismic anisotropy measurements show a distribution in agreement with a slab partitioning resulted from a differential slab retreat or plunging evolution and suggesting the presence of a vertical tear, probably evolved as a STEP tear (Govers and Wortel, 2005; Rosenbaum et al., 2008) located in correspondence of the transition between Northern and Southern Apennines. Indeed, anisotropy, supporting a toroidal mantle flow from the Adria to the Tyrrhenian side, supports also the presence of an interruption in the slab, of limited dimensions, located between 41.5° and 42° of latitude, in the southern part of the study region. The tear in this point is also in agreement with the interruption of the seismic anisotropy with Appenninic trend and the undeformed Adria mantle: the southern part of the slab stopped to retreat with respect to the northern one and did not further squeeze the mantle beneath it. Other data that supports the tear at this location are 1) the disagreement between SKS and Pn anisotropy; 2) the group of stations with a polar plot characterised by a particular amount of *E*-W fast polarisation directions in the SW quarter of back-azimuths (purple data in Fig. 3 and Figure 1SM in Supplementary Material). We imagine these E-W measurements as the flow through the slab; this feature is weaker further into the belt but delay times clearly increase towards the west, representing a streamflow variation. Last but not least, the narrow mantle flow that we draw using SKS measurements (Fig. 4B), is located exactly in correspondence with the only part of central to southern Apennines where lower CO2 degassing is recorded, in between of the northern Tuscan Roman and the southern Campanian degassing areas (Chiodini et al., 2004, 2020), meaning that conditions for gas to freely move upwards must be different.

The new geodynamic model we draw is only in part in agreement with those defined on the basis of tomographic images. For instance, anisotropy measurements confirm only the presence of the southern one of the two tears that Giacomuzzi et al. (2012) described under the Central Apennines. Concerning the northern one, that would be in agreement also with previous tomographies (e.g. Wortel and Spakman, 2000; Piromallo and Morelli, 2003; Benoit et al., 2011), we do not find any well developed pattern that sustains it at nearly 43° of latitude (Fig. 4B), out of the easternmost *E*-W data beneath the chain, that in an extreme interpretation may represent the asthenospheric "nose" that migrated following the portion of slab that retreated further east with respect to the southern one that stopped earlier its route. However, this hypothesised northern tear has been described recently in Chiarabba et al. (2020) as horizontal and shallow, within 100 km, still not evolved enough to favour a mantle flow, but related to the detachment of the oceanic lithosphere portion of the slab, now plunging down into the mantle. Following this interpretation, we guess this northern horizontal tear may well integrate with the vertical one we identified, probably it favours the presence of the E-W anisotropy in this peculiar position and an incipient flow of Adria mantle towards west.

In tomographic studies, mainly on d(Vp/Vs) maps, mantle upwelling and possible vertical mantle flows have been drawn on the Tyrrhenian side of the subduction system (Giacomuzzi et al., 2012). As already reported, shear wave splitting data are not the best to trace vertical patterns. However, a concentration of null measurements may indicate a vertical pattern, as for example a mantle upwelling (Long and Silver, 2009). Assuming this hypothesis, we observe the location of stations having a polar plot with only null measurements for eastern back-azimuth events and E-W to NW-SE measurements for opposite back-azimuths (Fig. 3, pink symbols): all of them are in the Tyrrhenian side of the study region, in particular along the inner part of the Northern Apennines arc where Giacomuzzi et al. (2012) hypothesised the occurrence of mantle upwelling.

6. Conclusions

This study describes the new shear wave splitting dataset carried out for the Central Apennines region. Most of the new measurements confirm the seismic anisotropy pattern already found for the Northern and Southern Apennines: a) a prevailing NW-SE seismic anisotropy beneath the high topography of the belt, interpreted as the mantle below the slab, deformed by the slab roll back, b) a N-S to NNE-SSW prevailing direction on the Adria side, considered as the undeformed Adria mantle, c) an E-W prevailing direction beneath the Tyrrhenian Sea, representing the mantle circulation above the slab and related to Tyrrhenian opening; d) a NW-SE anisotropy direction on the Tyrrhenian side, representing the asthenospheric mantle flow, originated below the Alpine slab and feeding the supra-mantle system of the Apennines.

The most interesting results are however some new interesting features in the seismic anisotropy distribution that shed more light on the deep structure of the Central Apennines. The typical NW-SE anisotropy direction beneath the chain is interrupted and absent in the southern part of the study region. In the same location, in the middle of the chain domain, typical Tyrrhenian E-W anisotropy and proper Adria mantle anisotropy directions are present; south of them a set of measurements with the pattern of a mantle flow from the Adria to the Tyrrhenian domain. The new measurements confirm the presence of a tear in the Apenninic slab, through which a toroidal mantle flow occurs. However, mantle circulation and flows, which the new measurements allowed us to interpret, are quite different from what has been defined in previous geodynamic models. The identified tear is vertical in this study and of limited dimension, as is the flow through it. In our final geodynamic sketch, this tear is functional for a differential slab retreat that is supported by the seismic anisotropy directions found here with respect to those characterising the Northern and the Southern Apennines. The large slab windows previously hypothesised for this region are still to come, as an evolution of the shallow horizontal tear identified by tomography and introduced in our sketch because located exactly where E-W directed seismic anisotropy is in its easternmost position.

Supplementary data to this article can be found online at https://doi.org/10.1016/j.tecto.2022.229549.

Credit author statement

Each of the three authors contributed to the preparation of this paper, starting from measurements to writing and discuss the final product.

Declaration of Competing Interest

The authors declare that they have no known competing financial interests or personal relationships that could have appeared to influence the work reported in this paper.

Data availability

Alla data used are available and described along with the paper.

Acknowledgements

We want to thank Claudio Chiarabba for sharing with us data from Giacomuzzi et al., 2012. Additionally our thanks go to Jeffrey Park for his helpful remarks in the revision process. This paper has been funded by the project INGV Pianeta Dinamico 2021-2022 Tema 4 KINDLE (grant no. CUP D53J19000170001) supported by the Italian Ministry of University and Research "Fondo finalizzato al rilancio degli investimenti delle amministrazioni centrali dello Stato e allo sviluppo del Paese, legge 145/2018" and by NEWTON (NEw Window inTO Earth's iNterior), ERC StG funded project (grant ID:758199).

References

Baccheschi, P., Margheriti, L., Steckler, M., 2007. Seismic anisotropy reveals focused mantle flow around the Calabrian slab (Southern Italy). Geophys. Res. Lett. 37, L05302. https://doi.org/10.1029/2006GL028899.

Baccheschi, P., Margheriti, L., Steckler, M.S., CAT/SCAN Seismology Team, 2008. SKS splitting in Southern Italy: Anisotropy variations in a fragmented subduction zone. Tectonophysics 462, 49–67.

Baccheschi, P., Margheriti, L., Steckler, M.S., Boschi, E., 2011. Anisotropy patterns in the subducting lithosphere and in the mantle wedge: a case study—the southern Italy subduction system. J. Geophys. Res. 116 (B08306).

Benoit, M.H., Torpey, M., Liszewski, K., Levin, V., Park, J., 2011. P and S wave upper mantle seismic velocity structure beneath the northern Apennines: New evidence for the end of subduction. Geochem. Geophys. Geosyst. 12 https://doi.org/10.1029/2010GC003428. Q06004.

Chiarabba, C., Jovane, L., DiStefano, R., 2005. A new view of Italian seismicity using 20 years of instrumental recordings. Tectonophysics 395 (3–4), 251–268.

Chiarabba, C., Giacomuzzi, G., Bianchi, I., Agostinetti, N.P., Park, J., 2014. From underplating to delamination-retreat in the northern Apennines. Earth Planet. Sci. Lett. 403, 108–116.

Chiarabba, C., Bianchi, I., De Gori, P., Piana Agostinetti, N., 2020. Mantle upwelling beneath the Apennines identified by receiver function imaging. Sci. Rep. 10, 19760. https://doi.org/10.1038/s41598-020-76515-2.

Chiodini, G., Cardellini, C., Amato, A., Boschi, E., Caliro, S., Frondini, F., Ventura, G., 2004. Carbon dioxide Earth degassing and seismogenesis in central and southern Italy. Geophys. Res. Lett. 31 (7).

Chiodini, G., Cardellini, C., Di Luccio, F., Selva, J., Frondini, F., Caliro, S., Rosiello, A., Beddini, G., Ventura, G., 2020. Correlation between tectonic CO2 Earth degassing and seismicity is revealed by a 10-year record in the Apennines, Italy. Sci. Adv. 6 (35), eabc2938.

Civello, S., Margheriti, L., 2004. Toroidal mantle flows around the Calabrian slab (Italy) from SKS splitting. Geophys. Res. Lett. 31, L10601. https://doi.org/10.1029/2004GL019607.

D'Agostino, N., Avallone, A., Cheloni, D., D'Anastasio, E., Mantenuto, S., Selvaggi, G., 2008. Active tectonics of the Adriatic region from GPS and earthquake slip vectors. J. Geophys. Res. 113, B12413. https://doi.org/10.1029/2008JB005860.

Dewey, J.F., Helman, M.L., Turco, E., Hutton, D.H.W., Knott, D., 1989. Kinematics of the western Mediterranean. In: Coward, M.P., Dietrich, D., Park, R.G. (Eds.), Alpine Tectonics, Geol. Soc. Spec. Publ, vol. 45, pp. 265–283.

Díaz, J., Gil, A., Gallart, J., 2013. Uppermost mantle seismic velocity and anisotropy in the Euro-Mediterranean region from Pn and Sn tomography. Geophys. J. Int. 192 (1), 310–325. https://doi.org/10.1093/gji/ggs016. January, 2013.

Faccenna, C., Becker, T.W., Lucente, F.P., Jolivet, L., Rossetti, F., 2001. History of subduction and back-arc extension in the Central Mediterranean. Geophys. J. Int. 145, 809–820.

Giacomuzzi, G., Chiarabba, C., De Gori, P., 2011. Linking the Alps and Apennines subduction systems: new constraints revealed by high-resolution teleseismic tomography. Earth Planet. Sci. Lett. 301 (3–4), 31–543.

Giacomuzzi, G., Civalleri, M., DeGori, P., Chiarabba, C., 2012. A 3D Vs model of the upper mantle beneath Italy: Insight on the geodynamics of Central Mediterranean. Earth Planet. Sci. Lett. 335–336, 105–120. https://doi.org/10.1016/j.epsl.2012.05.004.

Govers, R., Wortel, M.J.R., 2005. Lithosphere tearing at STEP faults: Response to edges of subduction zones. Earth Planet. Sci. Lett. 236, 505–523.

Jolivet, L., Faccenna, C., Piromallo, C., 2009. From mantle to crust: stretching the Mediterranean. Earth Planet. Sci. Lett. 285 (1–2), 198–209.

Long, M.D., Silver, P.G., 2009. Shear wave splitting and mantle anisotropy: Measurements, interpretations, and new directions. Surv. Geophys. 30 (4), 407–461.

Lopes, E., Long, M.D., Karabinos, P., Aragon, J.C., 2020. SKS splitting and upper mantle anisotropy beneath the southern New England Appalachians: Constraints from the dense SEISConn array. Geochem. Geophys. Geosyst. 21 https://doi.org/10.1029/2020GC009401 e2020GC009401.

Lucente, F.P., Chiarabba, C., Cimini, G.B., Giardini, D., 1999. Tomographic constraints on the geodynamic evolution of the Italian region. J. Geophys. Res. 104, 20,307–20,327. https://doi.org/10.1029/1999JB900147.

Lucente, F.P., Margheriti, L., Piromallo, C., Barruol, G., 2006. Seismic anisotropy reveals the long route of the slab through the western-Central Mediterranean mantle. Earth Planet. Sci. Lett. 241, 517–529. https://doi.org/10.1016/j.epsl.2005.10.041.

Malinverno, A., Ryan, W., 1986. Extension in the Tyrrhenian Sea and shortening in the Apennines as result of arc migration driven by sinking of the lithosphere. Tectonics 5, 227–245.

Margheriti, L., Lucente, F.P., Pondrelli, S., 2003. SKS splitting measurements in the Apenninic-Tyrrhenian domain (Italy) and their relation with lithospheric subduction and mantle convection. J. Geophys. Res. 108 (B4), 2218. https://doi.org/10.1029/2002JB001793.

Mediterranean Very Broadband Seismographic Network (MedNet), 1990. Istituto Nazionale di Geofisica e Vulcanologia (INGV). https://doi.org/10.13127/SD/FBBBTDTD6Q. January 1.

Patacca, E., Sartori, R., Scandone, P., 1990. Tyrrhenian Basin and Apenninic Arcs: Kinematic Relations Since Late Tortonian Times. Mem- orie della Societa Geologica Italiana, 45, pp. 425–451.

Picotti, V., Negri, A., Capaccioni, B., 2014. The geological origins and paleoceanographic history of the mediterranean region: tethys to present. In: Goffredo, S., Dubinsky, Z. (Eds.), The Mediterranean Sea. Springer, Dordrecht. https://doi.org/10.1007/978-94-007-6704-1_1.

Piromallo, C., Morelli, A., 2003. P wave tomography of the mantle under the Alpine-Mediterranean area. J. Geophys. Res. 108 (2065), B2. https://doi.org/10.1029/2002JB001757.

Plomerová, J., Margheriti, L., Park, J., Babuška, V., Pondrelli, S., Vecsey, L., Piccinini, D., Levin, V., Baccheschi, P., Salimbeni, S., 2006. Seismic anisotropy beneath the Northern Apennines (Italy): mantle flow or lithosphere fabric? Earth Planet. Sci. Lett. 247, 157–170. https://doi.org/10.1016/j.epsl.2006.1004.1023.

Pondrelli, S., Salimbeni, S., Baccheschi, P., Confal, J., Margheriti, L., 2022. Peeking inside the Deep Structure through Seismic Anisotropy: A Review in the Italian Region, under Review in Annals of Geophysics.

Rappisi, F., VanderBeek, B.P., Faccenda, M., Morelli, A., Molinari, I., 2022. Slab geometry and upper mantle flow patterns in the Central Mediterranean from 3D anisotropic P-wave tomography. J. Geophys. Res. Solid Earth 127. https://doi.org/10.1029/2021JB023488 e2021JB023488.

Reiss, M.C., Rümpker, G., 2017. SplitRacer: MATLAB Code and GUI for Semiautomated Analysis and Interpretation of Teleseismic Shear-Wave Splitting. Seismol. Res. Lett. 88 (2A), 392–409. https://doi.org/10.1785/0220160191.

Regional Seismic Network of North Western Italy [Data set]. International Federation of Digital Seismograph Networks. doi:10.7914/SN/GU.

Reiss, M.C., Long, M.D., Creasy, N., 2019. Lowermost mantle anisotropy beneath Africa from differential SKS-SKKS shear-wave splitting. J. Geophys. Res. Solid Earth 124 (8), 8540–8564.

Rete Sismica Nazionale (RSN), 2006. Istituto Nazionale di Geofisica e Vulcanologia (INGV), Italy. https://doi.org/10.13127/SD/X0FXNH7QFY.

Rosenbaum, G., Lister, G.S., 2004. Neogene and Quaternary rollback evolution of the Tyrrhenian Sea, the Apennines, and the Sicilian Maghrebides. Tectonics 23 (1).

Rosenbaum, G., Gasparon, M., Lucente, F.P., Peccerillo, A., Miller, M.S., 2008. Kinematics of slab tear faults during subduction segmentation and implications for Italian magmatism. Tectonics 27, TC2008. https://doi.org/10.1029/2007TC002143.

Salimbeni, S., Pondrelli, S., Margheriti, L., Levin, V., Park, J., Plomerova, J., Babuska, V., 2007. Abrupt change in mantle fabric across northern Apennines detected using seismic anisotropy. Geophys. Res. Lett. 34, L07308. https://doi.org/10.1029/2007GL029302.

Salimbeni, S., Pondrelli, S., Margheriti, L., Park, J., Levin, V., 2008. SKS splitting measurements beneath Northern Apennines region: a case of oblique trench-retreat. Tectonophysics 462, 68–82. https://doi.org/10.1016/j.tecto.2007.11.075.

Salimbeni, S., Pondrelli, S., Margheriti, L., 2013. Hints on the deformation penetration induced by subductions and collision processes: Seismic anisotropy beneath the Adria region (Central Mediterranean). J. Geophys. Res. 118 (11) https://doi.org/10.1002/2013jb010253, 2013JB010253.

Salimbeni, S., Pondrelli, S., Margheriti, L., Levin, V., Park, J., 2014. Looking for layered anisotropic structures in the mantle beneath the northern Apennines. J. Geodyn. 82, 39–51. Published: DEC 2014. https://doi.org/10.1016/j.jog.2014.09.001.

Salimbeni, S., Malusà, M.G., Zhao, L., Guillot, S., Pondrelli, S., Margheriti, L., et al., 2018. Active and fossil mantle flows in the western Alpine region unraveled by seismic anisotropy analysis and high-resolution P wave tomography. Tectonophysics 731, 35–47.

Salimbeni, S., Pondrelli, S., Molinari, I., Stipčević, J., Prevolnik, S., Dasović, I., the ALPARRAY-CASE working group, 2022. Seismic anisotropy across Adria plate, from the Apennines to the Dinarides. Front. Earth Sci. Sec. Solid Earth Geophys. https://doi.org/10.3389/feart.2022.881138.

Serpelloni, E., Anzidei, M., Baldi, P., Casula, G., Galvani, A., 2005. Crustal velocity and strain-rate fields in Italy and surrounding regions: new results from the analysis of permanent and non-permanent GPS networks. Geophys. J. Int. 161, 861–880. https://doi.org/10.1111/j.1365-246X.2005.02618.x.

Silver, P.G., Chan, W., 1991. Shear wave splitting and subcontinental mantle deformation. J. Geophys. Res. 96, 16,429–16,454.

Silver, P.G., Savage, M.K., 1994. The interpretation of shear wave splitting parameters in presence of two anisotropic layers. Geophys. J. Int. 119, 949–963.

Wortel, M.J.R., Spakman, W., 2000. Subduction and slab detachment in the Mediterranean-Carpathian region. Science 290, 1910–1917. https://doi.org/10.1126/science.290.5498.1910.